Polarization Splitter With Variable TE–TM Mode Converter Using Zn and Ni Codiffused $LiNbO_3$ Waveguides

Wen-Hao Hsu, *Student Member, IEEE*, Ko-Chun Lin, Jiun-Yun Li, Yir-Shyuan Wu, and Way-Seen Wang, *Member, IEEE*

***Abstract*—We propose and demonstrate a polarization splitter, in which the power ratio between transverse electric (TE) and transverse magnetic (TM) modes at two output arms can be electrically controlled. The mode-sorting effect and off-diagonal electrooptic coefficient of $LiNbO_3$ are utilized for polarization splitting and conversion, respectively. To simplify design and fabrication processes, we apply a newly developed zinc and nickel codiffusion technique in $LiNbO_3$, by which TE-, TM-, and randomly polarized waveguides can all be made by simply using different fabrication parameters. To lower the applied voltage, ridge structure is used to increase the overlap integral between electric and optical fields. Measured extinction ratios of polarization splitting are higher than 21 dB for TE mode and 18 dB for TM mode, and the applied voltage can be reduced by a factor of one-third with a ridge of height 3 μm. Finally an application example is proposed for future study.**

***Index Terms*—Electrooptic devices, integrated optics, optical polarization, optical waveguide components, ridge waveguides.**

I. Introduction

WAVEGUIDE polarization splitters are key components used in the polarization diversity receiver [1], optical gyroscope [2], and other photonic integrated circuits where different polarization states need to be separately processed. According to the operational principle, polarization splitters are divided into two categories. The first one is based on the mode interference, which manipulates the difference in phase velocity between two different polarizations. A typical illustration is using the directional coupler [3]–[5], in which the coupling lengths of TE and TM modes are carefully designed to achieve polarization splitting. This approach suffers from narrow wavelength range of operation and stringent tolerance of fabrication errors, such as lithographical misalignment and metallic lateral diffusion error. The second category is to use the mode-sorting effect [6], [7], mostly taking an asymmetric Y-branch to split different polarizations of the guided wave [8]–[11]. The basic idea of mode sorting effect is to differentiate two output arms of the Y-branch in their refractive indexes so that individual polarizations propagate preferentially along the arms with the closest propagation constant. This type of polarization splitter can be operated over a wide range of wavelength and is more tolerant to fabrication errors.

In these devices, however, output powers corresponding to TE and TM polarizations are determined by the state of polarization of input signal, and there is no mechanism to change their ratio at the output ends. When the state of polarization of the input signal varies with time and/or deviates from the designed state, the performance of entire optical circuit will be affected. In the polarization diversity receiver, for example, the available powers from the local oscillator at two polarizations, which are separated by a polarization splitter, must be controlled to be nearly equal; otherwise, the receiver performance will be degraded [12]. Many mechanisms may cause variations in the state of polarization of the input signal, such as propagating through long-haul fiber, polarization-dependent losses of cascading components, fabrication errors, etc. In this paper, we propose and demonstrate a polarization splitter in which the power ratio between different polarizations at two output arms can be electrically controlled, to provide a power tuning mechanism in polarization splitting. This device can be used in the polarization diversity receiver to equalize the available powers at two different polarizations from local oscillator and many other applications. In addition, Y-branch polarization splitters proposed in the literature used either specially designed waveguide dimensions [9] or heterogeneous structures combining different waveguide fabrication techniques [10], [11], which complicate the design and fabrication steps. In this work, for the design and fabrication simplicity, we use only one waveguide fabrication technique: a newly developed zinc and nickel codiffusion in $LiNbO_3$ to implement the polarization splitter. It is found that zinc and nickel codiffused waveguides have good process-dependent guiding property, which means the guided polarization can be selected by choosing proper fabrication parameters, and are suitable for using in polarization diversity optical circuits.

In the next section, we will first describe the configuration of proposed polarization splitter and its operational principle. Then in Section III, we will explain why we choose the zinc and nickel codiffused waveguides and their advantages compared to conventional $LiNbO_3$ waveguides. The design, fabrication processes, and discussion of experimental results are presented in Sections IV and V. In Section VI, the power control issue in the polarization diversity receiver and application of the proposed device are addressed.

Manuscript received May 21, 2004; revised October 11, 2004. This work is supported by National Science Council, Taipei, Taiwan, R.O.C., under Contract NSC 92-2215-E-002-009.

The authors are with the Graduate Institute of Electro-optical Engineering and the Department of Electrical Engineering, National Taiwan University, Taipei 106, Taiwan, R.O.C. (e-mail: wswang@cc.ee.ntu.edu.tw).

Digital Object Identifier 10.1109/JSTQE.2004.841463

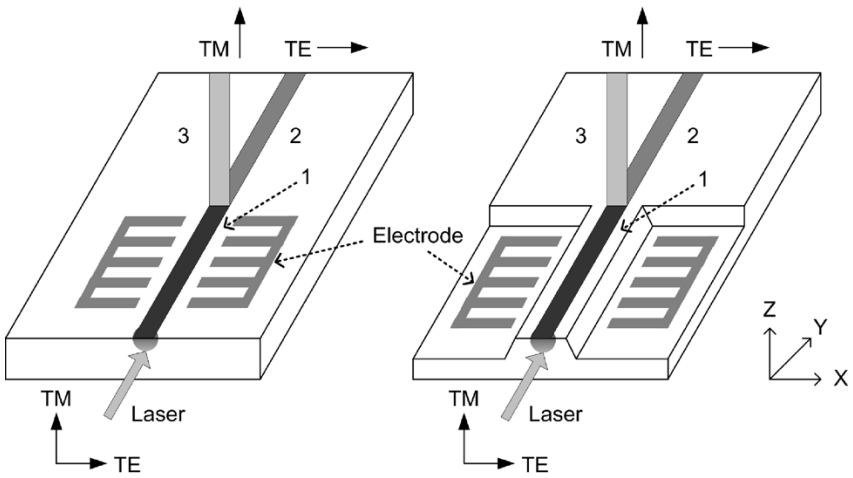

Fig. 1. Planar and ridged configurations of the proposed device. The substrate orientations are both in Z-cut and Y-propagation. There are three different sections (marked by 1, 2, and 3) of waveguide to form the Y branch.

II. Polarization Splitter With Variable TE–TM Mode Converter

Fig. 1 shows the planar and ridged configurations of the proposed polarization splitter with variable TE–TM mode converter on Z-cut, Y-propagation $LiNbO_3$ substrates. The device consists of three waveguide sections: 1) the input section supporting both TE and TM modes between a pair of finger-type electrodes; 2) a TE branch following the input branch straightly and supporting only a TE-mode wave; and 3) a TM branch bending from the input waveguide and supporting only a TM-mode wave. The widths of all waveguides are designed for single mode propagation at the operating wavelength. The Y-branch constructed by these three sections forms a mode-sorting-based polarization splitter, and the input section along with the finger-type electrode forms a TE–TM mode converter, in which TE–TM mode conversion can be induced by applying electric field along direction X because of the off-diagonal electrooptic coefficient r_{51} of $LiNbO_3$. The coupling coefficient κ and conversion efficiency η of the TE–TM mode converter can be written as [13]

$$\kappa = \gamma \left(\frac{2\pi}{\lambda}\right) n^3 r_{51} \left(\frac{V}{d}\right) \tag{1}$$

$$\eta = \sin^2 \left[\gamma \left(\frac{2\pi}{\lambda}\right) n^3 r_{51} \left(\frac{V}{d}\right) L\right] \tag{2}$$

where V is the applied voltage, d is the interelectrode gap, n is the geometric average of refractive indexes at TE and TM polarizations, λ is the wavelength, γ is the overlap integral between the applied electric field and the optical field, and L is the electrode length. The purpose of using a ridge structure is to increase the overlap integral, which had been proposed in the study of a Mach–Zehnder modulator [14]. Because of the large birefringence of Z-cut $LiNbO_3$, the mode conversion efficiency is highly wavelength dependent and requires a finger-type electrode of period Λ satisfying the phase matching condition

$$\frac{2\pi}{\lambda} \times |n_{\mathrm{TE}} - n_{\mathrm{TM}}| = \frac{2\pi}{\Lambda} \tag{3}$$

where n_{TE} and n_{TM} are the refractive indexes of TE and TM modes, respectively. Therefore, when the signal enters the input section, its TE and TM components can be varied by changing voltage on the electrode, and, after passing through the Y-branch polarization splitter, adjustable power ratio at two output arms can be obtained.

In the proposed device, we apply the Y-branch structure because it is more tolerant to fabrication error and wavelength variation. Besides, the use of single-polarization waveguides for TE and TM output arms has several advantages.

1) High extinction ratio can be achieved without special design for the waveguide dimensions [9].
2) It has good performance even for multimode propagation [11].
3) It has potential for wide-angle polarization splitter design [15].

Several experiments have been carried out by using single-polarization waveguides for one or both output arms [10], [11]. Although the extinction ratios were shown to be reasonably high, the fabrication processes were complicated, since different waveguide fabrication techniques in $LiNbO_3$, such as titanium indiffusion (TI), annealed proton exchange (APE), magnesium-induced lithium out-diffusion (MILO), nickel indiffusion (NI), etc., must be combined to form a heterogeneous Y-branch. Moreover, different diffusion characteristics among different fabrication techniques can cause higher branching loss due to propagation mode mismatch [16]. To avoid these problems, we resort to a newly developed zinc and nickel codiffusion process and found it to be very suitable for the fabrication of homogenous polarization splitters with single-polarization output arms.

III. Zinc and Nickel Codiffused Waveguides

The most widely used fabrication techniques for $LiNbO_3$ waveguides include TI and APE, which are well known for low propagation loss and high index change, respectively. However, to fabricate a homogenous polarization splitter with single-polarization output arms in the proposed device, neither TI nor APE is suitable, since their guided polarizations are

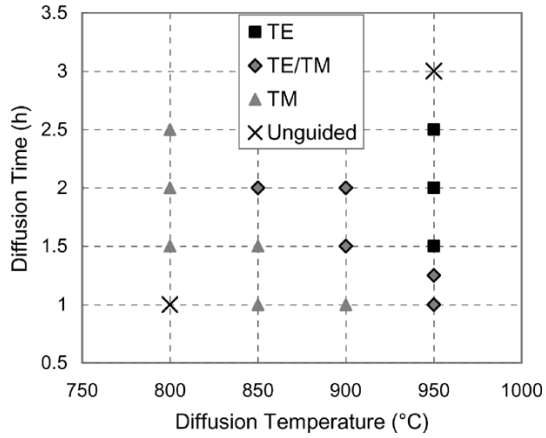

Fig. 2. Guided polarization versus diffusion temperature and time for thicknesses of zinc and nickel of 750 and 200 Å, respectively.

fixed: single-polarization waveguide cannot be made by TI; random- or ordinary-polarization waveguide cannot be made by APE.

We previously combined the zinc and nickel as the diffusion sources for waveguide fabrication and successfully demonstrated a heterogeneous polarization splitter with high extinction ratios [17]. It was experimentally found that the zinc and nickel codiffused waveguide has a good process-dependent guiding property, which is also possessed by NI [18], better optical confinement than NI [19], and is free of lithium outdiffusion. To demonstrate the process-dependent guiding property, several waveguides are fabricated under different diffusion temperatures, diffusion times, and thicknesses of zinc and nickel. The guided polarization versus diffusion temperature and time is shown in Fig. 2 for the zinc and nickel thicknesses of 750 and 200 Å, respectively. At low diffusion temperature and short diffusion time, only TM mode (extraordinary wave on Z-cut $LiNbO_3$) is guided. When the diffusion temperature and time rise, both TM and TE waves can be guided simultaneously. If the diffusion temperature and time are high enough (950 °C for more than 1.5 h), only TE mode (ordinary wave on Z-cut $LiNbO_3$) can be guided. Fig. 3 shows output mode profiles of TM- and TE-polarized waveguides and their fabrication parameters. To measure the polarization selectivity of the singly polarized waveguide, the polarization extinction ratio ξ is defined as

$$\xi = 10 \log \left(\frac{P_1}{P_2} \right) \tag{4}$$

where P_1 is the power of guided polarization and P_2 is the power of the other polarization when the input is at 45° polarization. In Fig. 3(a), where only TM mode is guided, ξ is measured to be 26 dB. In Fig. 3(b), only TE mode is guided, and ξ is measured to be 28 dB. For both profiles, full-widths at half-maximum (FWHMs) in the vertical and horizontal directions are about 9 and 7 μm, respectively. We see that single-polarization waveguides at both polarization states with high polarization extinction ratio and good optical confinement can be fabricated by the zinc and nickel codiffusion process. Therefore, it is used to fabricate the proposed device.

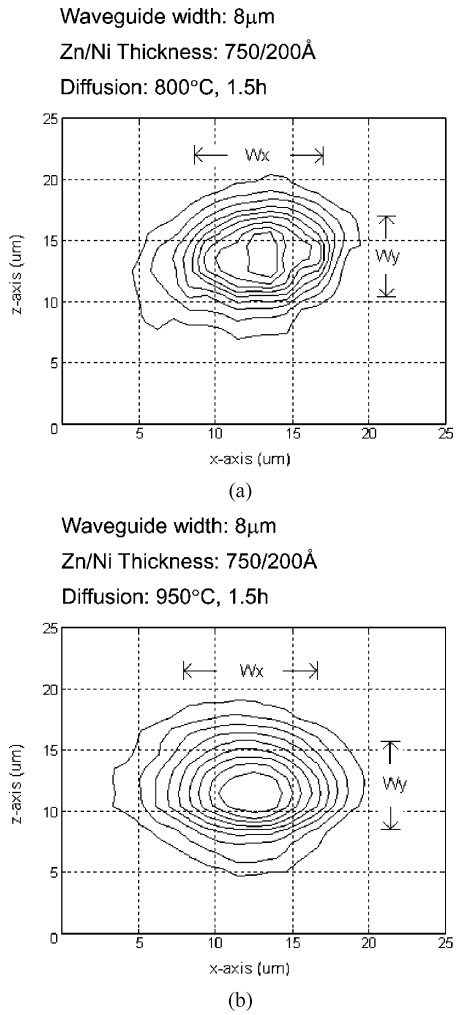

Fig. 3. Optical fields and fabrication conditions of singly polarized waveguides. (a) TM polarized. (b) TE polarized. W_x and W_y, the FWHMs, are 9 and 7 μm, respectively.

TABLE I
WAVEGUIDE FABRICATION PARAMETERS OF DIFFERENT GUIDED POLARIZATIONS

Polarization (Mode)	Thickness (Ni)	Thickness (Zn)	Diffusion Temp.	Diffusion Time
TE & TM	200Å	750Å (1^{st}) 1000Å (2^{nd})	950°C	1.5 h
TE	200Å	750Å	950°C	1.5 h
TM	200Å	750Å	800°C	1.5 h

IV. EXPERIMENT

Fabrication process parameters for different waveguide sections in the proposed polarization splitter are listed in Table I. Waveguides at different sections are all 8 μm wide for single-mode propagation at $\lambda = 1.55\,\mu$m. The branching angle is 0.5°, and the total device length is about 1 cm, including 6-mm-long input guide and 4-mm-long branching guides. Fabrication steps are illustrated in Fig. 4. First, the ridge is formed by the wet etching method [20] before any waveguide is fabricated (this step is skipped for the planar device). The wet etching process

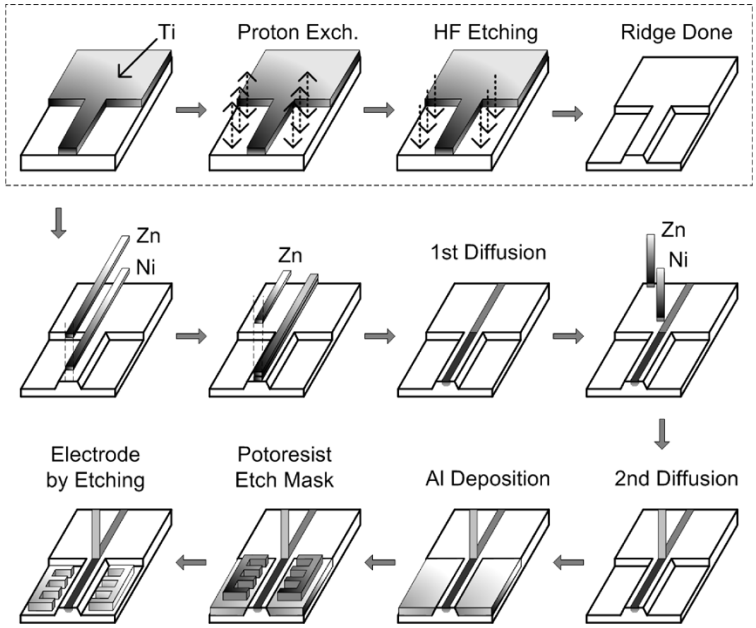

Fig. 4. Fabrication steps of the proposed polarization splitter. The inset illustrates the wet etching process on Z-cut $LiNbO_3$.

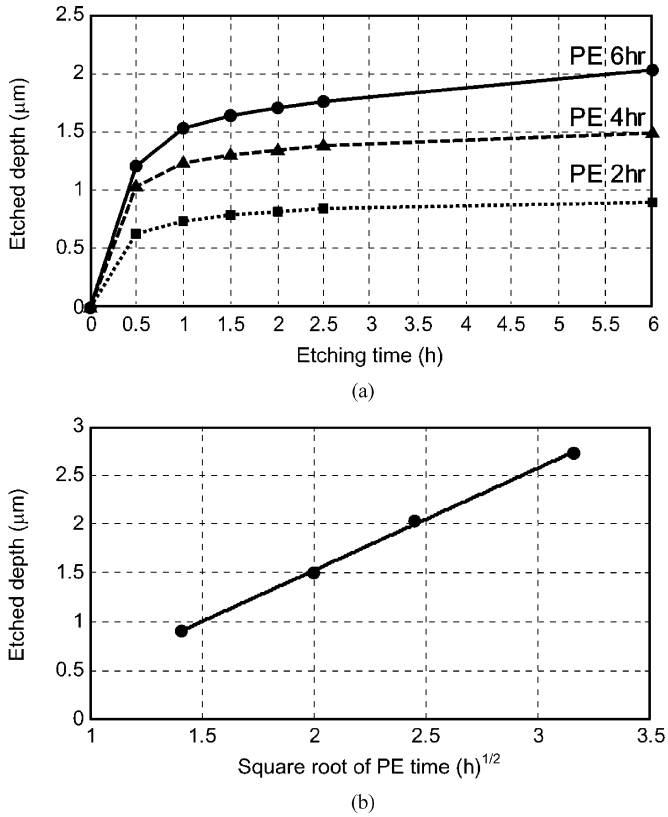

Fig. 5. Etched depth versus (a) etching time and (b) square root of proton exchange time.

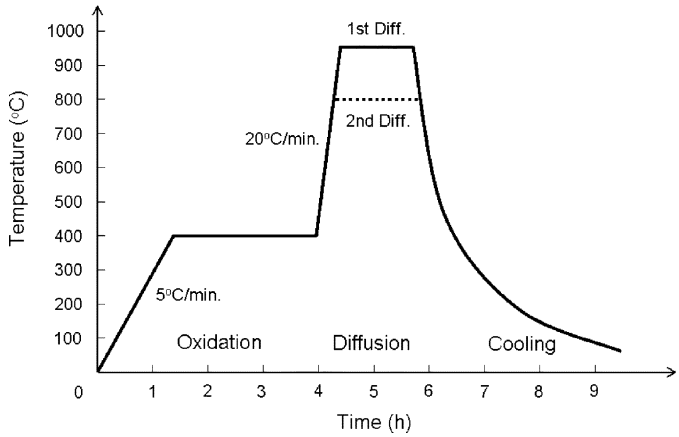

Fig. 6. Temperature rising curve for zinc and nickel codiffusion process.

is illustrated in the inset of Fig. 4. To etch the Z-cut $LiNbO_3$, a layer of 4500-Å-thick titanium is deposited on the substrate as the mask for proton exchange. The sample is then submerged in benzoic acid at 240 °C for several hours (depending on the ridge height) and, subsequently, etched with hydrofluoric acid to reveal the ridge structure. We have fabricated two ridges of heights 2 and 3 μm. Fig. 5(a) and (b), respectively, show the etching depth versus etching time and the linear relation between the etching depth and square root of proton exchange time, which satisfies the diffusion model [21]. Second, a strip of 200-Å-thick nickel and 750-Å-thick zinc is sequentially thermally deposited onto the input and TE-output sections. Then another 1000-Å-thick zinc strip is added onto the input section. The strip is then diffused in the furnace with a temperature rising curve as shown in Fig. 6 to form the input and TE-output sections. The stop at 400 °C for 2 h as shown in Fig. 6 is for the oxidation of zinc metal, which is necessary to prevent the metallic strip from distortion due to the abruptly rising temperature. Next, a 200-Å-thick nickel and a 750-Å-thick zinc metallic strip are deposited to make the TM bending branch and then the diffusion is repeated. Note that although the input and TE-output sections are diffused twice, we did not observe any influence of the guiding property, including the polarization extinction ratio and optical confinement, because of relatively lower temperature (800 °C) of the second diffusion. Then we fabricate the periodic electrode onto the input section for TE–TM mode conversion. The electrode period is determined by the phase matching condition described in (3). For $LiNbO_3$ at $\lambda = 1.55$ μm, the estimated $|n_{\mathrm{TE}} - n_{\mathrm{TM}}|$ is 0.0734 leading to the electrode period

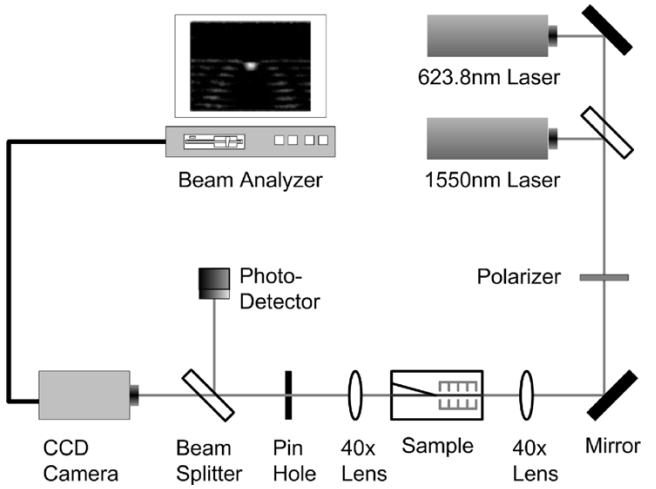

Fig. 7. Measurement setup.

$\Lambda = 21\ \mu$m. The electrode length is set to be 4 mm, and the interelectrode gap is 12 μm. Finally, a 3000-Å-thick aluminum is deposited and a periodic-electrode patterned photoresist is lithographically transformed to form the etch mask. The sample is then etched in 85%, 70 °C phosphoric acid for 20 s to pattern the periodic electrodes.

V. Results and Discussion

The fabricated devices are characterized by the measurement setup shown in Fig. 7. Since the distributed-feedback laser at $\lambda = 1.55\ \mu$m is invisible, a He–Ne laser at 0.6328 μm is coupled for easy alignment. The sample is excited by end-fire coupling, and the output optical field contour profiles are captured by a charge-coupled-device camera. Output fields of the polarization splitter are shown in Fig. 8(a)–(c) with an input light at TM, TE, and 45° polarization, respectively. The extinction ratios of TE and TM modes are defined as

$$\xi_{\mathrm{TE}} = 10\log\left(\frac{P_{\mathrm{TE(TE-Branch)}}}{P_{\mathrm{TE(TM-Branch)}}}\right) \tag{5}$$

$$\xi_{\mathrm{TM}} = 10\log\left(\frac{P_{\mathrm{TM(TM-Branch)}}}{P_{\mathrm{TM(TE-Branch)}}}\right) \tag{6}$$

where the numerators in logarithm represent the power of the "correct" polarization component, and the denominators represent the power of "wrong" polarization component. The measurement shows that ξ_{TE} and ξ_{TM} are higher than 21 and 18 dB, respectively, for both planar and ridge structures. Then we apply voltage to the mode converter; the measured results are shown in Fig. 9. For the planar structure, when 100 V is applied, 40% of the power (tunability) at one output arm (polarization) is converted to the other one. We compare the applied voltage with that reported in [13], in which 40% is reached at 9 V for $\lambda = 0.5995\ \mu$m, $d = 5\ \mu$m, $L = 6$ mm. According to (2), the applied voltage is, to the first order, proportional to design parameters as

$$V \propto \frac{\lambda d}{\gamma L}. \tag{7}$$

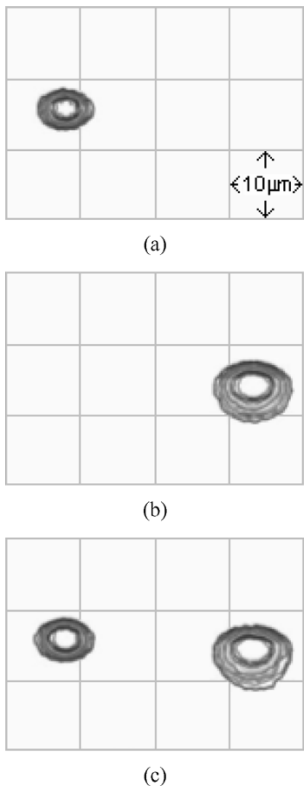

Fig. 8. Output field contours with different input polarizations. (a) TM. (b) TE. (c) 45°.

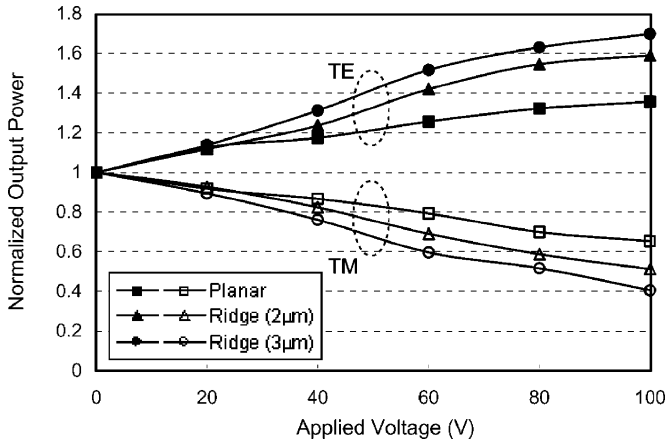

Fig. 9. Measured power tunability versus applied voltage.

If the overlap integral γ is the same, the expected voltage for a 40% tunability in our case ($\lambda = 1.55\ \mu$m, $d = 12\ \mu$m, $L = 4$ mm) is estimated to be about 84 V. The higher voltage required in our work can be induced by the decrease in γ under long wavelength operation, which is also observed in [22]. To obtain higher overlap integral, we measure ridged devices, and results are also shown in Fig. 9. For a ridge height of 2 μm, a tunability of about 60% is obtained at 100 V, and only 60 V is required for the same tunability as that of the planar device. The applied voltage is reduced by a factor of about 1/3 due to the increased overlap integral of the ridge structure. Recent results have shown that a ridge of height 3 μm provides more flexible power tuning range than that of 2 μm does. Future optimization of the ridge height for a lower applied voltage is of great interest. Other existing methods such as depositing longer electrodes or

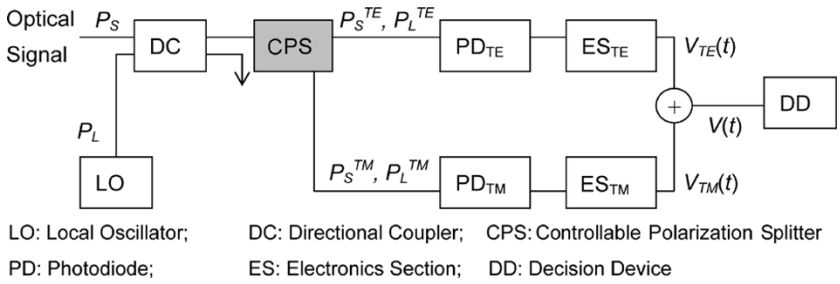

Fig. 10. Block diagram of a polarization diversity receiver with controllable polarization splitter.

etching a ridge closer to the input waveguide can also be used to reduce the applied voltage significantly.

VI. Application in the Polarization Diversity Receiver

Fig. 10 shows the block diagram of a polarization diversity receiver with the proposed polarization splitter with controllable output power ratio (called a controllable polarization splitter in the figure). The usage and benefit of replacing the conventional noncontrollable polarization splitter with a controllable one is described as follows.

Assume that the available powers of the TE and TM component of the optical signal at the photodiodes are

$$P_S^{\mathrm{TE}} = \beta^2 P_S \tag{8}$$
$$P_S^{\mathrm{TM}} = (1-\beta^2) P_S \tag{9}$$

where P_S is the available power of the optical signal at the photodiodes and β^2 represents the power ratio of the TE component in P_S. Note that β is time varying because standard optical fiber does not maintain the polarization state. The design goal of the polarization diversity receiver is to remove the influence of β on receiver performance.

In addition, assume that the available powers of the TE and TM component of the local oscillator signal at the photodiodes are

$$P_L^{\mathrm{TE}} = \alpha^2 P_L \tag{10}$$
$$P_L^{\mathrm{TM}} = (1-\alpha^2) P_L \tag{11}$$

where P_L is the available power of the local oscillator signal at the photodiodes and α^2 represents the power ratio of the TE component in P_L. Note that in real cases, $\alpha^2 \neq 0.5$, i.e., $P_L^{\mathrm{TE}} \neq P_L^{\mathrm{TM}}$, because the available power from the local oscillator laser and characteristics of components prior to the photodiodes, including optical waveguides, directional couplers, and polarization splitter, are polarization dependent.

One can write the voltages detected by two photodiodes at the intermediate frequency to be proportional to [1]

$$V_{\mathrm{TE}}(t) = 4P_S P_L \left\{\beta^2\alpha^2 M'(t)\cos[\Delta\phi(t)] + n_1(t)\right\} \tag{12}$$
$$V_{\mathrm{TM}}(t) = 4P_S P_L \left\{(1-\beta^2)(1-\alpha^2)M'(t)\cos[\Delta\phi(t)] + n_2(t)\right\} \tag{13}$$

where $M'(t)$ is the modulated signal, $\Delta\phi(t)$ is the phase difference of two signals, and $n_1(t)$ and $n_2(t)$ represent the noise terms. Thus, the sum of $V_{\mathrm{TE}}(t)$ and $V_{\mathrm{TM}}(t)$ yields the detected signal entering the decision device can be written as

$$V(t) = 4P_S P_L \left\{(1-\beta^2-\alpha^2+2\beta^2\alpha^2)M'(t)\cos[\Delta\phi(t)] + n(t)\right\} \tag{14}$$

where $n(t) = n_1(t) + n_2(t)$. We see that there is a power-dependent factor $(1-\beta^2-\alpha^2+2\beta^2\alpha^2)$ influencing the detected signal $V(t)$. For different values of α^2, the parameter $(1-\beta^2-\alpha^2+2\beta^2\alpha^2)$ is plotted as a function of β^2 in Fig. 11. Note that only when $\alpha^2 = 0.5$, that is, $P_L^{\mathrm{TE}} = P_L^{\mathrm{TM}}$, the polarization diversity receiver is truly independent of the state of polarization of the optical signal, which is the design goal of this receiver. Once α^2 deviates from the value 0.5, the detected signal $V(t)$ in (14) will be dependent on β, as shown in Fig. 11.

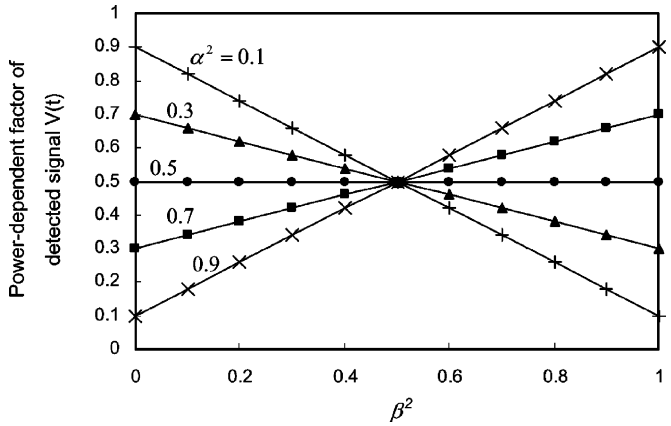

Fig. 11. Power-dependent factor $(1-\beta^2-\alpha^2+2\alpha^2\beta^2)$ of the detected signal in (14) as a function of β^2 for different values of α^2.

To solve this problem, the proposed polarization splitter is applied into the receiver, as shown in Fig. 10, to control the local oscillator power at different polarizations. After the local oscillator laser, which may be a semiconductor or waveguide laser with unbalanced TE/TM components, and other optical components are fabricated, one can adjust the power ratio of TE and TM modes from the local oscillator until they are equal at the photodiodes. With the power control mechanism of the polarization splitter, the receiver is guaranteed to be independent of the input signal's state of polarization, thus operating with the optimal performance.

VII. Conclusion

For the first time to our knowledge, polarization splitters integrated with variable TE–TM mode converters in planar and ridge structures are proposed and demonstrated. We apply the

newly developed zinc and nickel codiffused $LiNbO_3$ waveguide to fabricate the polarization splitter with singly polarized output arms on Z-cut $LiNbO_3$. The zinc and nickel codiffused waveguide is found to have a good process-dependent guiding property, and both randomly polarized and singly polarized waveguides with a polarization extinction ratio greater then 26 dB are demonstrated in this work. Experimental results show that the extinction ratios of polarization splitter are no less than 21 and 18 dB for TE and TM modes, respectively. It is shown that the applied voltage is reduced by a factor of one-third by using the ridge structure and can be further lowered by optimizing ridge heights or simply using a longer electrode. Application of the proposed device to keep optimal performance for polarization diversity receivers in coherent detection is also illustrated. Potential usages in other polarization diversity circuits, such as a polarization stabilizer [23] or polarization switch, will be of great interest in the future.

REFERENCES

[1] B. Glance, "Polarization independent coherent optical receiver," *J. Lightw. Technol.*, vol. 5, no. 2, pp. 274–276, Feb. 1987.

[2] W. J. Minford, R. Depaula, and G. A. Bogert, "Interferometric fiber optical gyroscope using a novel 3×3 integrated optic polarizer/splitter," in *Dig. Conf. Optical Fiber Sensors*, 1988, pp. 385–392.

[3] M. Kobayashi, H. Terui, and K. Egashira, "An optical TE–TM mode splitter," *Appl. Phys. Lett.*, vol. 32, pp. 300–302, 1979.

[4] D. Yap, L. M. Johnson, and G. W. Pratt Jr., "Passive $Ti:LiNbO_3$ channel waveguide TE–TM mode splitter," *Appl. Phys. Lett.*, vol. 44, pp. 583–585, 1984.

[5] R. C. Twu, C. C. Huang, and W. S. Wang, "TE–TM mode splitter with heterogeneously coupled Ti-diffused and Ni-diffused waveguides on Z-cut lithium niobate," *Electron. Lett.*, vol. 36, pp. 220–221, Feb. 2000.

[6] H. Yajima, "Dielectric thin-film optical branching waveguide," *Appl. Phys. Lett.*, vol. 22, pp. 647–649, 1973.

[7] W. K. Burns and A. F. Milton, "Mode conversion in planar-dielectric separating waveguides," *IEEE J. Quantum Electron.*, vol. 11, no. 1, pp. 32–39, Jan. 1975.

[8] M. Masuda and G. L. Yip, "A passive TE/TM mode splitter using a $LiNbO_3$ branching waveguide," *Appl. Phys. Lett.*, vol. 37, pp. 20–22, 1980.

[9] J. J. G. M. van der Tol and J. H. Laarhuis, "A polarization splitter on $LiNbO_3$ using only titanium diffusion," *J. Lightw. Technol.*, vol. 9, no. 7, pp. 879–886, Jul. 1991.

[10] N. Goto and G. L. Yip, "A TE–TM mode splitter in $LiNbO_3$ by proton exchange and Ti diffusion," *J. Lightw. Technol.*, vol. 7, no. 10, pp. 1567–1574, Oct. 1989.

[11] P. K. Wei and W. S. Wang, "Novel TE–TM mode splitter on lithium niobate using nickel indiffusion and proton exchange techniques," *Electron. Lett.*, vol. 30, pp. 35–37, Jan. 1994.

[12] J. Hankey, J. Urquhart, A. J. Moseley, C. Edge, M. J. Wale, M. Owen, and S. J. Pike, "Balanced polarization diversity receiver using hybrid assembly techniques for optical coherent multichannel systems," *Electron. Lett.*, vol. 27, pp. 1935–1937, Oct. 1991.

[13] R. C. Alferness, "Efficient waveguide electro-optic TE $\Leftrightarrow$ TM mode converter/wavelength filter," *Appl. Phys. Lett.*, vol. 36, pp. 513–515, 1980.

[14] E. L. Wooten, K. M. Kissa, A. Yi-Yan, E. J. Murphy, D. A. Lafaw, P. F. Hallemeier, D. Maack, D. V. Attanasio, D. J. Fritz, G. J. McBrien, and D. E. Bossi, "A review of lithium niobate modulators for fiber-optic communication systems," *IEEE J. Sel. Topics Quantum Electron.*, vol. 6, no. 1, pp. 69–82, Jan./Feb. 2000.

[15] Y. P. Liao and R. C. Lu, "Design and fabrication of wide-angle TE–TM mode splitter in lithium niobate," *IEEE J. Sel. Topics Quantum Electron.*, vol. 6, no. 1, pp. 88–93, Jan./Feb. 2000.

[16] S. R. Park and B.-H. O, "Novel design concept of waveguide mode adapter for low-loss mode conversion," *IEEE Photon. Technol. Lett.*, vol. 13, no. 7, pp. 675–677, Jul. 2001.

[17] J. Y. Li, W. H. Hsu, and W. S. Wang, "A TE–TM mode splitter using annealed proton exchange and zinc/nickel co-diffusion waveguides," in *Tech. Dig. CLEO/Pacific Rim*, vol. 1, 2001, pp. 94–95.

[18] Y. P. Liao, D. J. Chen, R. C. Lu, and W. S. Wang, "Nickel-diffused lithium niobate optical waveguide with process-dependent polarization," *IEEE Photon. Technol. Lett.*, vol. 8, no. 4, pp. 548–550, Apr. 1996.

[19] Y. P. Liao and R. C. Lu, "TE-pass polarizers with NI-NIPE-NI structure in z-cut $LiNbO_3$," *Electron. Lett.*, vol. 35, pp. 1465–1467, Aug. 1999.

[20] F. Laurell, J. Webjorn, G. Arviddson, and J. Holmberg, "Wet etching of proton-exchanged lithium niobate—A novel processing technique," *J. Lightw. Technol.*, vol. 10, no. 11, pp. 1606–1609, Nov. 1992.

[21] J. L. Jackel, C. E. Rice, and J. J. Veselka, "Proton exchange for high-index waveguides in $LiNbO_3$," *Appl. Phys. Lett.*, vol. 41, pp. 607–608, 1982.

[22] N. A. Sanford, J. M. Connors, and W. A. Dyes, "Simplified Z-propagating DC bias stable TE–TM mode converter fabricated in Y-cut lithium niobate," *J. Lightw. Technol.*, vol. 6, no. 6, pp. 898–902, Jun. 1988.

[23] W. Y. Hwang, M. C. Oh, H. Park, J. H. Ahn, S. G. Han, and H. G. Kim, "Polarization stabilizer using a polarization splitter and a thermooptic polymer waveguide device," *IEEE Photon. Technol. Lett.*, vol. 10, no. 12, pp. 1736–1738, Dec. 1998.

Wen-Hao Hsu (S'02) was born in Taipei, Taiwan, R.O.C., in 1976. He received the B.S. degree in electrical engineering and the M.S. degree in electrooptical engineering in 1999 and 2001, respectively, both from National Taiwan University, Taipei. He is currently working toward the Ph.D degree at National Taiwan University.

He joined the Integrated Optics Laboratory, National Taiwan University since 1998. His research interests include electrooptic waveguide devices, optical waveguide sensors, and short-wavelength dielectric waveguides.

Ko-Chun Lin received the M.S. degree in electrooptical engineering from National Taiwan University, Taiwan, in 2002. His research interest includes the design and fabrication of integrated optical waveguide devices on lithium niobate.

Jiun-Yun Li was born in Taipei, Taiwan, R.O.C., on Nov. 28, 1975. He received the B.S. degree in electrical engineering and the M.S. degree in electrooptical engineering from National Taiwan University, Taipei, in 1998 and 2000, respectively. He is currently working toward the Ph.D. degree in the Department of Electrical and Computer Engineering at the University of Maryland, College Park.

After two years of military life, he was with Academia Sinica, Taipei. His research interests include integrated-optic devices, silicon-based optoelectronic and electronic devices, and quantum computing.

Yir-Shyuan Wu received the M.S. degree in electrooptical engineering from the National Taiwan University, Taipei, in 1998.

Her research interest includes the design and fabrication of integrated optical waveguide devices on lithium niobate.

Way-Seen Wang (M'84) was born on March 11, 1948, in Taipei, Taiwan, R.O.C. He received the B.S. degree in electrical engineering from National Taiwan University, Taipei, in 1970, and the M.S. and Ph.D. degrees from the University of Southern California, Los Angeles, in 1975 and 1979, respectively.

Since 1971, he has been with the Department Of Electrical Engineering, National Taiwan University. In 1984, he became a Full Professor. His current research interest includes the design and fabrication of integrated optical waveguide devices.